Brain, Behavior, & Immunity - Health 26 (2022) 100555

Contents lists available at ScienceDirect

Brain, Behavior, & Immunity - Health

journal homepage: www.editorialmanager.com/bbih/default.aspx

Conserved YKL-40 changes in mice and humans after postoperative delirium

Jennifer David-Bercholz [a,1], Leah Acker [a,1], Ana I. Caceres [a], Pau Yen Wu [a], Saanvi Goenka [a], Nathan O. Franklin [b], Ramona M. Rodriguiz [b], William C. Wetsel [b,c,d], Michael Devinney [a], Mary Cooter Wright [a], Henrik Zetterberg [e,f,g,h,i], Ting Yang [j], Miles Berger [a], Niccolò Terrando [a,d,k,*]

[a] Department of Anesthesiology, Duke University Medical Center, Durham, NC, United States
[b] Department of Psychiatry and Behavioral Sciences, Mouse Behavioral and Neuroendocrine Analysis Core Facility, Duke University Medical Center, Durham, NC, United States
[c] Department of Neurobiology, Duke University Medical Center, Durham, NC, United States
[d] Department of Cell Biology, Duke University Medical Center, Durham, NC, United States
[e] Department of Psychiatry and Neurochemistry, Institute of Neuroscience and Physiology, The Sahlgrenska Academy at the University of Gothenburg, Mölndal, Sweden
[f] Clinical Neurochemistry Laboratory, Sahlgrenska University Hospital, Mölndal, Sweden
[g] Department of Neurodegenerative Disease, UCL Institute of Neurology, Queen Square, London, UK
[h] UK Dementia Research Institute at UCL, London, UK
[i] Hong Kong Center for Neurodegenerative Diseases, Clear Water Bay, Hong Kong, China
[j] Department of Medicine, Duke University Medical Center, Durham, NC, United States
[k] Department of Immunology, Duke University Medical Center, Durham, NC, United States

ARTICLE INFO

Keywords:
Aging
Attention
Biomarkers
Delirium
YKL-40
Surgery

ABSTRACT

Delirium is a common postoperative neurologic complication among older adults. Despite its prevalence (14%–50%) and likely association with inflammation, the exact mechanisms that underpin postoperative delirium are unclear. This project aimed to characterize systemic and central nervous system (CNS) inflammatory changes following surgery in mice and humans. Matched plasma and cerebrospinal fluid (CSF) samples from the "Investigating Neuroinflammation Underlying Postoperative Brain Connectivity Changes, Postoperative Cognitive Dysfunction, Delirium in Older Adults" (INTUIT; NCT03273335) study were compared to murine endpoints. Delirium-like behavior was evaluated in aged mice using the 5-Choice Serial Reaction Time Test (5-CSRTT). Using a well established orthopedic surgical model in the FosTRAP reporter mouse we detected neuronal changes in the prefrontal cortex, an area implicated in attention, but notably not in the hippocampus. In aged mice, plasma interleukin-6 (IL-6), chitinase-3-like protein 1 (YKL-40), and neurofilament light chain (NfL) levels increased after orthopedic surgery, but hippocampal YKL-40 expression was decreased. Given the growing evidence for a YKL-40 role in delirium and other neurodegenerative conditions, we assayed human plasma and CSF samples. Plasma YKL-40 levels were similarly increased after surgery, with a trend toward a greater postoperative plasma YKL-40 increase in patients with delirium. However, YKL-40 levels in CSF decreased following surgery, which paralleled the findings in the mouse brain. Finally, we confirmed changes in the blood-brain barrier (BBB) as early as 9 h after surgery in mice, which warrants more detailed and acute evaluations of BBB integrity following surgery in humans. Together, these results provide a nuanced understanding of

Abbreviations: CNS, *central nervous system*; CSF, *cerebrospinal fluid*; 5-CSRTT, *5-Choice Serial Reaction Time Test*; YKL-40, *chitinase-3-like protein 1*; IL-6, *interleukin-6*; NfL, *neurofilament light chain*; BBB, *blood-brain barrier*; CAM, *Confusion AssessmentMethod*; AD, *Alzheimer's disease*; TRAP, *Targeted Recombination in Active Populations*; 4-OHT, *4-hydroxytamoxifen*; IHC, *immunohistochemistry*; PBS, *phosphate-buffered saline*; PFA, *paraformaldehyde*; GFAP, *glial fibrillary acidic protein*; ROI, *regions of interest*; ELISA, *enzyme-linked immunosorbent assay*; SIMOA, *single molecule array*; MMSE, *mini-mental status exam*; PLC, *prelimbic cortex*.

* Corresponding author. Department of Anesthesiology, Duke University Medical Center, Durham, NC, United States.
E-mail address: niccolo.terrando@duke.edu (N. Terrando).
[1] Co-first author.

https://doi.org/10.1016/j.bbih.2022.100555
Received 26 September 2022; Accepted 11 November 2022
Available online 17 November 2022

neuroimmune interactions underlying postoperative delirium in mice and humans, and highlight translational biomarkers to test potential cellular targets and mechanisms.

1. Introduction

Delirium is a neurologic complication characterized by changes in cognition, attention, and arousal (Wilson et al., 2020). Aging is the most prominent risk factor for postoperative delirium; however, we currently do not understand how aging contributes to the onset of delirium mechanistically. Delirium is observed frequently after routine surgical procedures such as orthopedic surgery, which comprises 4 of the 5 most common surgical procedures in US hospitals (Fingar et al., 2014). Postoperative delirium can affect up to 50% of older adults (Inouye et al., 2014), and adds $33.3 billion to annual US healthcare costs (Gou et al., 2021), rendering its impact on patients, families, and overall health care highly significant.

Delirium is clinically evaluated by neuropsychological testing, with the Confusion Assessment Method (CAM) being the most widely used research tool (De and Wand, 2015). In clinical practice, a shorter form of the CAM, the 3-min CAM (3D-CAM), is often used (Marcantonio et al., 2014). Like the long-form CAM, the 3D-CAM has been validated against psychiatric interviews, the "gold standard" (Marcantonio et al., 2014). Further, the 3D-CAM has good overall agreement with the long-form CAM, as it assesses delirium based on the same 4 domains: 1) acute change and/or a fluctuating disease course, 2) inattention, 3) disorganized thinking, and/or 4) altered level of consciousness (Marcantonio et al., 2014; Vasunilashorn et al., 2020).

Aside from cognitive testing, more recent efforts have been devoted to biomarker discovery with the intent of establishing predictive molecular signatures that can be related to worse postoperative neurocognitive outcomes. Part of this effort is occurring in parallel with the development and validation of animal models that can reliably interrogate cellular and molecular mechanisms that underpin delirium and other acute perioperative neurocognitive disorders (Evered et al., 2022).

We have been interested in modeling key features of delirium in rodents, and have focused on different types of surgery performed in older adults as well as orthopedic trauma, arthroplasty surgery, and various mechanisms of injury (eg, falls) common in seniors (Masutani et al., 2020). Using these models, we and others have described a key role for pro-inflammatory cytokines in triggering neuroinflammation, including changes in glial activation (microglia and astrocytes), and cytokines associated with the behavioral features found in patients with delirium. In particular, we have focused on inattention as one of the key clinical domains (Velagapudi et al., 2019; Wang et al., 2020). In addition, our murine model has revealed changes in blood-brain barrier (BBB) permeability after surgery (Yang, 2022), a complication that has now been observed in the clinic (Taylor et al., 2022).

YKL-40 (chitinase-3-like protein 1) is a glycoprotein that is secreted by multiple cell types including macrophages, vascular smooth muscle cells, astrocytes, and microglia, and has been implicated in a variety of cancers and more recently in neurodegenerative disorders (Llorens et al., 2017). YKL-40 is often upregulated in the CSF of patients with prodromal Alzheimer's disease (AD) (Craig-Schapiro et al., 2010) and mild cognitive impairments (MCI), suggesting its putative role as an early "immune" biomarker. However, its upregulation has not been described in other dementias, possibly due to its diffuse role across multiple immune cell types including reactive astrocytes. Notably, YKL-40 plasma levels, which are increased after lower extremity orthopedic surgery in older adults (Vasunilashorn et al., 2021), have been proposed as a strong biomarker predictor of postoperative delirium (Vasunilashorn et al., 2022). However, the origin of plasma YKL-40 after surgery remains unclear. Further, it is not yet known whether elevated plasma levels of YKL-40 levels after surgery reflect an increase in systemic and/or central levels of YKL-40.

The present studies are focused on evaluating systemic and CNS changes in YKL-40 in aged mice after surgery. Using a parallel human cohort of 22 non-neurologic non-cardiac surgery patients aged ≥60 years from the INTUIT study (Berger et al., 2019) with matched plasma and CSF samples, we investigated the notion that YKL-40 responses are conserved in both mice and humans.

2. Methods

2.1. Animals

2.1.1. Animal characteristics and care

Adult (17–24 months old) male C57BL/6 mice (The Jackson Laboratory, Bar Harbor, ME, USA) were used in these experiments. Male and female Fos-TRAP2; Ai14 mice (3–4 months old; gift from Dr Fan Wang) (DeNardo et al., 2019) were also used. All mice were housed 3–5 per cage under controlled temperature and humidity conditions with a 14:10-h light:dark cycle. Mice were fed rodent chow (Prolab RMH3500, Autoclavable; LabDiet, St. Louis, MO, USA) with *ad libitum* access to food and water. All experiments were conducted under an approved protocol by the Institutional Animal Care and Use Committee at Duke University Medical Center, and according to the guidelines described in the National Science Foundation "Guide for the Care and Use of Laboratory Animals" (2011).

2.1.2. Fos-TRAP2; Ai14 and 4-OHT administration

The Targeted Recombination in Active Populations (TRAP) system is a tool that creates permanent genetic access to neurons activated by any stimulation (Guenthner et al., 2013). In the recently developed FosTRAP mouse, Cre recombinase is stimulated to produce permanent expression of td-tomato when neurons are activated in the presence of tamoxifen (DeNardo et al., 2019). FosTRAP mice were housed individually with at least 2 environmental enrichments for approximately 10 days before 4-hydroxytamoxifen (4-OHT) administration day (Cat# H6278, Sigma-Aldrich, St. Louis, MO, USA). The 4-OHT was dissolved in 100% ethanol to make a 20 mg/mL stock solution, and samples were aliquoted and frozen at −20 °C. On administration day, an aliquot of the 4-OHT solution was added to sunflower seed oil (Cat #S5007; Sigma-Aldrich, St. Louis, MO, USA), and heated to 50 °C to remove the ethanol, yielding a final 4-OHT solution of 10 mg/mL. Thirty minutes before start of surgery, 50 mg/kg 4-OHT was administered (ip) to mice undergoing orthopedic surgery and to naïve controls. Sevoflurane anesthesia (Covetrus, North America, Dublin, OH, USA) was administered to mice during surgery and to non-operated naïve controls. All mice were returned to their individual cages, minimizing any source of distress prior to termination.

2.1.3. Murine orthopedic surgery

Tibial facture was performed as described (Velagapudi et al., 2019). Mice were anesthetized with isoflurane via a low-flow digital anesthesia system (SomnoSuite apparatus; Kent Scientific Corporation, Torrington, CT, USA). Body temperature was maintained at 36.5 °C ± 0.6 °C using a homoeothermic pad system (Kent Scientific Corporation). The muscles were dissociated following an incision on the left hind paw. A 0.38-mm stainless steel pin was inserted into the tibial intramedullary canal, followed by osteotomy, and the incision was closed with 6–0 Prolene suture. Naïve controls did not undergo surgery.

2.1.4. Tissue collection and immunohistochemistry

2.1.4.1. Dissection and tissue preparation. For immunohistochemistry

(IHC), mice were euthanized under deep isoflurane anesthesia via trans-cardiac perfusion with 50 mL ice-cold 0.1 M phosphate-buffered saline (PBS; pH 7.4), followed by 50 mL ice-cold 4% paraformaldehyde in PBS (PFA). Brains were dissected from the skull, placed in 4% PFA overnight, washed the next day with PBS, placed in a 30% sucrose solution for 3 days, and then stored in optimal cutting temperature (OCT) compound at −80 °C until sectioning. The post-fixed brains were coronally cut with a cryostat (Leica CM, 1950; Leica Biosystems, Deer Park, IL, USA) in 45-μm (IHC) or 80-μm sections (FosTRAP brains).

2.1.4.2. Immunostaining. Free-floating sections were washed 3 times with PBS (15 min each), blocked for 1 h in blocking buffer (2.5% BSA, 0.3% Triton X-100 PBS), and incubated overnight at 4 °C with the primary antibody in the blocking buffer. The following antisera were used: rabbit anti-AQ-4 (1:500, #AB3594; Millipore, Sigma Aldrich, St. Louis, MO, USA), rabbit anti-YKL-40 (1:300, #PA5-43746; ThermoFisher Scientific, Waltham, MA, USA), goat anti-CD31 (1:500, #AF3628; R&D Systems, Minneapolis, MN, USA), rabbit anti-NeuN (1:1000, #ABN78; Millipore, Sigma-Aldrich, St. Louis, MO, USA), and mouse anti-glial fibrillary acidic protein (GFAP; 1:500, #G3893; Sigma-Aldrich, St. Louis, MO, USA). The next day sections were washed 3 times with the blocking buffer (15 min each), and subsequently incubated for 1 h at room temperature with the secondary antibody in the blocking buffer. The secondary antibodies consisted of donkey anti-rabbit 647 (1:1000, #AB150075; ABCAM, Cambridge, MA, USA), donkey anti-mouse 594, anti-goat 488, and anti-rabbit 488 (each 1:1000, #A21203, #A11055, #A21206, respectively; Invitrogen, and ThermoFisher Scientific, Waltham, MA, USA). Lastly, sections were washed 2 times with PBS (10 min each), and finally mounted onto slides covered with DAPI mounting media (#F6057; Sigma-Aldrich, St. Louis, MO, USA).

2.1.4.3. Imaging. Image stacks of the regions of interest (ROIs) were acquired with a 20× or 40× objective on a Zeiss inverted 880 confocal microscope. For Fos-TRAP2 samples, the sections were acquired with a Dragonfly 505 spinning-disk confocal microscope with a 10× or 20× objective for imaging. Maximum intensity projections were analyzed using FIJI software by threshold analysis after background subtraction. Automatic algorithms were determined to match the best cell morphology and to decrease the noise/signal ratio, as described previously (Healy et al., 2018).

2.1.5. Tissue collection, RNA extraction, cDNA synthesis, and PCR

2.1.5.1. Tissue collection. Animals were euthanized under deep isoflurane anesthesia via trans-cardiac perfusion with 50 mL ice-cold 0.1 M phosphate buffered saline only. After perfusion, brains were removed from the skull, and hippocampi were microdissected on a metallic plate on ice, snap-frozen in liquid nitrogen, and stored at −80 °C until further use.

2.1.5.2. RNA extraction and cDNA synthesis. Total RNA was isolated from the tissue homogenates of each sample using the Qiagen RNeasy Lipid Tissue Mini Kit (Qiagen, Germantown, MD, USA). The homogenization of all the tissues was performed in a NextAdvance bullet blender at 4 °C in Eppendorf Safe-Lock tubes. The cDNA synthesis was performed with 200 ng RNA immediately after RNA isolation, using a High-Capacity Reverse-Transcription Kit (Applied Biosystems, Foster City, CA, USA) and following the manufacturer's instructions. The RNA quality and quantity were determined with a NanoDrop 1000 Spectrophotometer (Qiagen, Germantown, MD, USA) with RIN values above 8.0.

2.1.5.3. Real-time PCR (qPCR). TaqMan® Gene Expression Assays (Applied Biosystems, Foster City, CA, USA) were used for expression assessment using reactions containing 10 μL of TaqMan® Fast Advanced Master Mix (2×), 1 μL of the specific TaqMan® assay, 5 μL cDNA, and DNAase/RNAase-free water to adjust the reaction to a 20 μL volume. Thermal cycling was performed on a Real-Time PCR system Light Cycler 480 (Roche, Indianapolis, IN, USA) in 384-well plates. Each reaction was performed in triplicate, and normalized to endogenous 18 S gene expression. The CT value of each well was determined using LightCycler 480 software, and the mean of the triplicates was calculated. The relative quantification was determined using the ΔΔCT method (Livak and Schmittgen, 2001). TaqMan® Gene Expression Assays used the following: Aqp4: Mm00802131_m1; Ykl40: Mm00801477_m1; 18 S rRNA Mm03928990_g1; IL-1β: Mm00434228_m1; Cd31: Mm01242576_m1; ZO1: Mm01320638_m1; Ocln: Mm00500912_m1; Cldn5: Mm00727012_s1.

2.1.6. 5-Choice Serial Reaction Time Test (5-CSRTT)

The 5-CSRTT was conducted as previously described (Velagapudi et al., 2019; Wang et al., 2020) with minor modifications. The food magazine dispensed single food rewards (20 mg sucrose cocoa-based pellet; BioServ, Flemington, NJ, USA), and testing occurred daily with 25 trials/day until a criterion of a 1.5-sec stimulus duration was achieved. Mice were trained on the task, their baseline responses were recorded, and post-surgical testing began one day after surgery or following treatment of the naïve controls.

2.1.7. Plasma collection and analyses

2.1.7.1. Plasma collection. Blood was collected 24 h after tibial fracture from mice via cardiac puncture with a heparinized syringe under terminal anesthesia. The blood was centrifuged at 6500 RPM (Sorvall legend, micro 21 R centrifuge, Thermo-Scientific, Waltham, MA, USA) for 10 min at 4 °C, and the plasma was stored at −80 °C before analysis.

2.1.7.2. ELISA. ELISA kits were used to quantitate the mouse plasma levels of YKL-40 (1:40 dilution, #AB238262; ABCAM, Cambridge, MA, USA), IL-6 (1:4–1:2 dilution, #KMC0061; ThermoFisher Scientific, Waltham, MA, USA), and NfL (1:4 dilution, #103186; Quanterix, Middlesex Turnpike, MA, USA). These samples were evaluated following the manufacturer's instructions.

2.2. Human patients

2.2.1. Subject inclusion and treatment

The 22 human patients (Table 1) were derived from a subset of patients in a larger cohort study: Investigating Neuroinflammation Underlying Postoperative Brain Connectivity Changes, Postoperative Cognitive Dysfunction, Delirium in Older Adults (INTUIT). Briefly,

Table 1
Cohort characteristics.

	All (n = 22)
Age (years), mean (SD)	68 (5)
Male sex, n (%)	11 (50)
Years of education, median (Q1, Q3)	16 (14, 17)
Baseline Mini-Mental Status Exam Score, median (Q1, Q3)	28 (25, 29)
***APOE4* Carrier, n (%)**	9 (41)
ASA physical status, n (%)	
2	7 (32)
3	13 (59)
4	2 (9)
Surgical service, n (%)	
Thoracic	4 (18)
General surgery	7 (32)
Gynecology	3 (14)
Orthopedics	4 (18)
Urology	4 (18)
Surgery duration (min incision to end procedure), median (Q1, Q3)	137 (74, 168)

INTUIT is a prospective observational single-site cohort study of patients ≥ 60 years of age who are undergoing non-neurologic non-cardiac surgery with a scheduled duration >2 h. Exclusion criteria includes incarceration, inadequate English fluency, and anticoagulant use that would preclude lumbar punctures. INTUIT has no cognitive exclusion criteria. The INTUIT sub-cohort in this analysis was selected according to age and surgery-type match between subjects who were *APOE4* carriers and non-carriers. Hence, this sub-cohort represented an *APOE4* carrier-enriched group relative to the overall INTUIT cohort. The present experiment was approved by the Duke Health Institutional Review Board, and was registered on clinicaltrials.gov (NCT03273335) (Berger et al., 2019). All participants, or legally authorized representatives, provided written informed consent prior to study participation.

2.2.2. Baseline cognitive assessment and delirium assessment

Subjects underwent a cognitive battery preoperatively, as described (Berger et al., 2019). This battery included the mini-mental status exam (MMSE) - a commonly used cognitive screening tool. The 3D-CAM was administered preoperatively to establish a baseline, and was then administered twice daily throughout the postoperative hospitalization period to capture the fluctuations in mental status that characterize delirium. The 3D-CAM assessment was scored for the presence or absence of delirium as well as delirium severity, using the "raw" scoring method (Vasunilashorn et al., 2020).

2.2.3. Human plasma and CSF collection

Blood samples were collected before and 24 h after surgery using standard procedures including a clean puncture, or draw-back, from an arterial or venous line with waste drawn prior to sample collection to account for fluid in the tubing and to prevent sample dilution. Blood was collected in EDTA-containing tubes, and centrifuged at 3500 RPM for 15 min at 4 °C. Plasma was aliquoted into 1.5-mL microcentrifuge tubes (VWR International, West Chester, PA, USA) using low-binding pipette tips (Genesee Scientific, San Diego, CA, USA), and stored at −80 °C before analysis. CSF samples were collected via lumbar puncture using sterile technique before and 24 h after surgery, as described (Nobuhara et al., 2020).

2.2.4. ELISA

2.2.4.1. Assay of YKL-40 in plasma. YKL-40 concentrations in plasma (YKL-40, 1:160, ab255719, ABCAM, Cambridge, MA, USA) were quantitated in samples collected prior to surgery and 24 h after surgery from the same subject, following the manufacturer's instructions.

2.2.4.2. Assay of YKL-40 in CSF. YKL-40 concentrations in the CSF were quantitated in one round of analyses with one batch of reagents using a commercially available ELISA kit (R&D Systems, Minneapolis, MN, USA), following the manufacturer's instructions. The assay was conducted by a board-certified laboratory technician who was blinded to the clinical data.

2.3. Statistics

Mice data are presented as means and standard errors of the mean (SEMs). Performance on the 5-CSRTT was collected from the same mouse over time and the data were analyzed with repeated-measures ANOVA (RMANOVA) followed by Bonferroni-corrected pair-wise comparisons. In separate experiments, differences between control and surgical mice were compared by student's *t*-tests. Human data are presented as means and standard deviation of the mean (SD) or median and quartile 1,3. Biomarker data were analyzed using *t*-tests for normally distributed data or Wilcoxon rank-sum tests (WRS) for data that failed the Shapiro-Wilk test for normality. Mouse data were analyzed with GraphPad 9.4.1 Prism (GraphPad Software, San Diego, CA, USA) and IBM SPSS 27 programs (IBM, Chicago, IL, USA). Human data were analyzed using SAS 9.4 programs (SAS Institute Inc, Cary, NC, USA) by a statistician who had no role in clinical data collection or biospecimen processing. All hypothesis testing was 2-tailed, and statistical significance was set at $p \leq 0.05$.

3. Results

3.1. Postoperative delirium-like behavior (attention task) in aged mice

To assess attention processes, mice were pre-trained on the 5-CSRTT to a criterion of 1.5 s for presentation of the visual stimulus. Upon reaching criterion, animals were assigned to two groups: sham surgical controls and mice that underwent knee surgery. Twenty-four hours after sham or knee surgery, the animals were re-tested in the 5-CSRTT and daily testing continued for 4 additional days. At 48 and 24 h prior to surgery, Mice performed at levels approximately of 81% and 85% correct responses, respectively (Fig. 1A). Following surgery, attention performance for the mice that had knee surgery was significantly lower on days 1 ($p = 0.018$), 4 ($p = 0.046$), and 5 ($p = 0.050$) compared to the sham controls. For the sham group, their levels of performance pre-sham were not significantly different from those on any of the days post-sham surgery. For the knee surgery group, attention performance on all post-surgery days was significantly reduced compared to the 24 h time-point prior to knee surgery (p-values≤0.014).

As a further evaluation of responses on the 5-CSRTT, we examined the latency to respond to the 1.5 s visual stimulus. Recall that the mouse had a maximum of 5 s to respond to this stimulus. 48 and 24 h prior to sham or knee surgery, the latencies to respond were approximately 2.3 and 2 s, respectively (Fig. 1B). After these times, responses in the knee surgery group were significantly higher on day 1 ($p = 0.002$), 2 ($p = 0.004$), 3 ($p = 0.001$), 4 ($p = 0.026$), and 5 ($p = 0.008$) than the sham controls. For the sham controls, no differences were found among any of the pre- or post-sham surgery days. In contrast for the knee-surgery group, the latencies to respond on all days post-surgery were significantly prolonged relative to the 24 h time-point prior to their surgery (p-values≤0.047). Collectively, these results indicate that the animals that underwent knee surgery were significantly impaired immediately after surgery and on several additional days post-surgery compared to the sham controls. While the knee surgery animals took much longer to respond to the 1.5 s visual stimulus than the sham mice, this longer latency suggests that attention processes may have been slowed in the surgical group.

3.2. Neuronal activity changes after surgery

To determine the brain areas that were most affected by the surgery, we used FosTRAP mice. Notably, an examination of FosTRAP expression revealed activation of the prefrontal area and particularly, the prelimbic cortex (PLC), a key region involved in attentional processing (Squire et al., 2013; Bichot et al., 2015), in mice subjected to tibial surgery (Fig. 1C). Higher magnification showed that Td-tomato + staining co-localized with NeuN + staining, confirming that surgery activated Fos expression in neurons of the prelimbic area (Fig. 1D-E). Indeed, quantification of Td-tomato + expression (ie, Fos + cells) in the medial prelimbic area showed a significant increase in surgical mice: Naïve mean: 1.317 (SEM: 0.5665), Surgery mean: 4.395 (SEM: 0.6852); Student's *t*-test; ($p = 0.0085$; MD = 3.078, 95% CI [1.028, 5.128]) (Fig. 1F). Interestingly, no significant treatment effect was observed in the hippocampus (data not shown).

3.3. Astrocyte impairment and YKL-40 expression in the CNS after surgery in mice

We and others have previously described glial changes, particularly microglial activation after surgery (Velagapudi et al., 2019; Wang et al.,

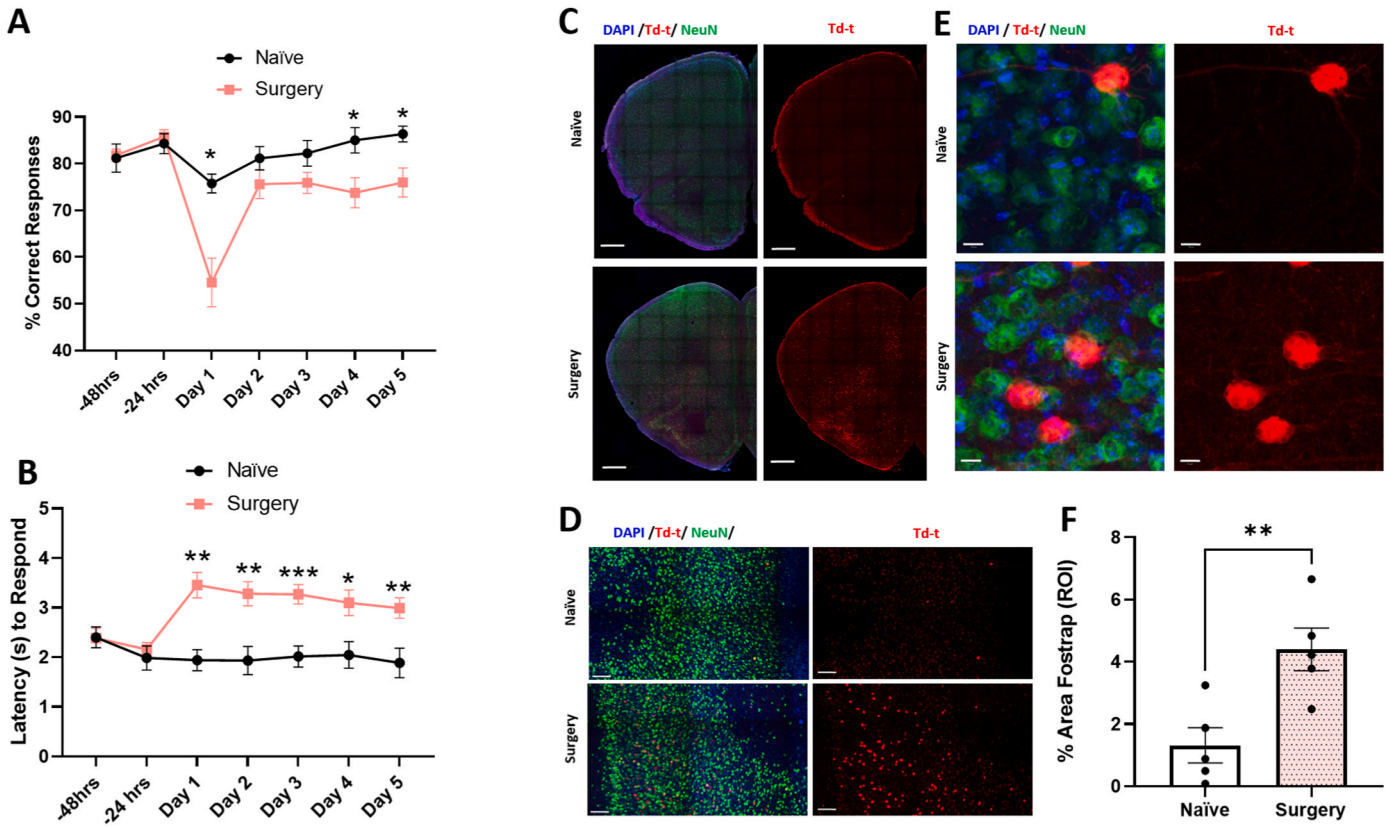

Fig. 1. Delirium-like behavior and neuronal changes associated with surgery. Aged mice were trained on the 5-CSRTT, an attention task. A) The surgery group made fewer correct responses on this attention task than the sham controls at 24 h and at 4 and 5 days post-fracture. A RMANOVA found the within subjects effects of days [F6,108) = 10.005, p < 0.001] and the days by treatment interaction [F (6,108) = 3.800, p = 0.002], as well as the between subjects effect of treatment [F (1,18) = 4.994, p = 0.038] to be significant. B) The latency to respond in the 5-CSRTT was prolonged on days 1–5 post-surgery in the group that received the tibial fracture compared to the sham controls. A RMANOVA detected significant differences in days [F (6,108) = 2.281, p = 0.041], treatment [F (1,18) = 12.125, p = 0.003], and in the days by treatment interaction [F (6,108) = 4.440, p < 0.001]. N = 6 mice sham, N = 14 mice surgical. C, D, E) Representative pictures of FosTRAP activation in FosTrap2 mice after surgery and naïve control mice shown in half brain, the PLC, and with higher magnification of the PLC. F) Quantification data from panel D revealed that surgery increases FosTRAP activation in the PLC when compared to naïve controls. Data are expressed as mean ± SEM. Analyses were performed as follows: RMANOVA, Bonferroni's *post-hoc* analysis, and Unpaired Student's *t*-test, *p < 0.05, **p < 0.01, ****p < 0.001, sham *vs.* knee-surgery mice. Scale bars: 500 μm for C), 100 μm for D) and 10 μm for E). PLC: prelimbic cortex.

2020). Here, we focused on astrocytes, the most abundant cell type in the brain. Note, this cell type has not been extensively examined in this model. Expression of the astrocyte marker GFAP, known to be low in naïve conditions in the PLC brain region (David et al., 2019), was found to be the same in the present study (data not shown); therefore, immunohistochemical evaluation was not possible in this brain region. Due to this limitation, we assessed changes in GFAP and YKL-40 in the hippocampal dentate gyrus (Fig. 2A).

At 24 h after surgery, YKL-40 protein immuno-reactivity expression in the dentate gyrus was significantly decreased in surgery mice relative to controls: Naïve mean: 2.826 (SEM: 0.1888), Surgery mean: 2.198 (SEM: 0.2202); Student's *t*-test; (p = 0.0481; MD = −0.6281, 95% CI [−1.25, −0.006]) (Fig. 2B). *Ykl*-40 mRNA expression was also examined, and was found to be decreased at this time point by −0.355 log 2 (fold changes) (Fig. 2C).

To corroborate the loss of YKL-40 expression, and due to its regulation by the macrophage-released pro-inflammatory mediator interleukin-1β (IL-1β) (Breyne et al., 2018), we also measured expression of *Il-1β* mRNA to confirm neuroinflammation, which increased by 0.806 log2 (fold changes), as previously described in this model (Fig. 2C).

3.4. YKL-40 changes in human CSF after surgery

To determine whether our YKL-40 results in mice could be replicated in humans, we assayed the levels of this protein in the CSF of human patients undergoing surgery. Overall, YKL-40 levels in human CSF were reduced at 24 h after surgery relative to the levels in the same patients before surgery (Median [Q1, Q3] pre-op: 149.2 ng/mL [121.1, 169.1], 24 h post-op: 136.7 ng/mL [121.9, 166.8]; Wilcoxon Rank Sum Test; p = 0.030) (Fig. 2D), and when considering individual subject trajectories before and after surgery (Fig. 2E). However, there was no difference in the post-surgical change between patients with or without delirium, (Median [Q1, Q3] with delirium −3.2 [−4.0, 3.6], without delirium −3.3 [−11.3, −1.7]; Wilcoxon Rank Sum Test; p = 0.601) (Fig. 2F).

3.5. Increased plasma YKL-40 after surgery in both mice and humans

Next we measured YKL-40 in plasma and CSF samples collected at the same time from the same human subjects. In human plasma, YKL-40 levels increased from before to 24 h after surgery (Mean pre-op: 72.3 ng/mL (SD: 76.6), 24 h post-op: 279.7 ng/mL (SD: 203.3); Student's *t*-test; p = 0.001) (Fig. 3A,B). In addition, we observed a potential trend toward a greater increase in YKL-40 from pre-op to 24-h post-op among patients with delirium compared to patients without delirium. The average YKL-40 increase (SD) for those without delirium was 156.7 ng/mL (SD: 164.7) vs 336.2 ng/mL (SD: 277.6) for those with delirium (Student's *t*-test; p = 0.114) (Fig. 3C). Similarly, mouse YKL-40 plasma levels at 24 h were higher following tibial fracture vs sham treatment: Naïve mean: 26.55 ng/mL (SEM: 2.265), Surgery mean: 50.36 ng/mL (SEM: 4.153); Student's *t*-test; (p = 0.0002; MD = 23.81, 95% CI [14.18, 33.45])

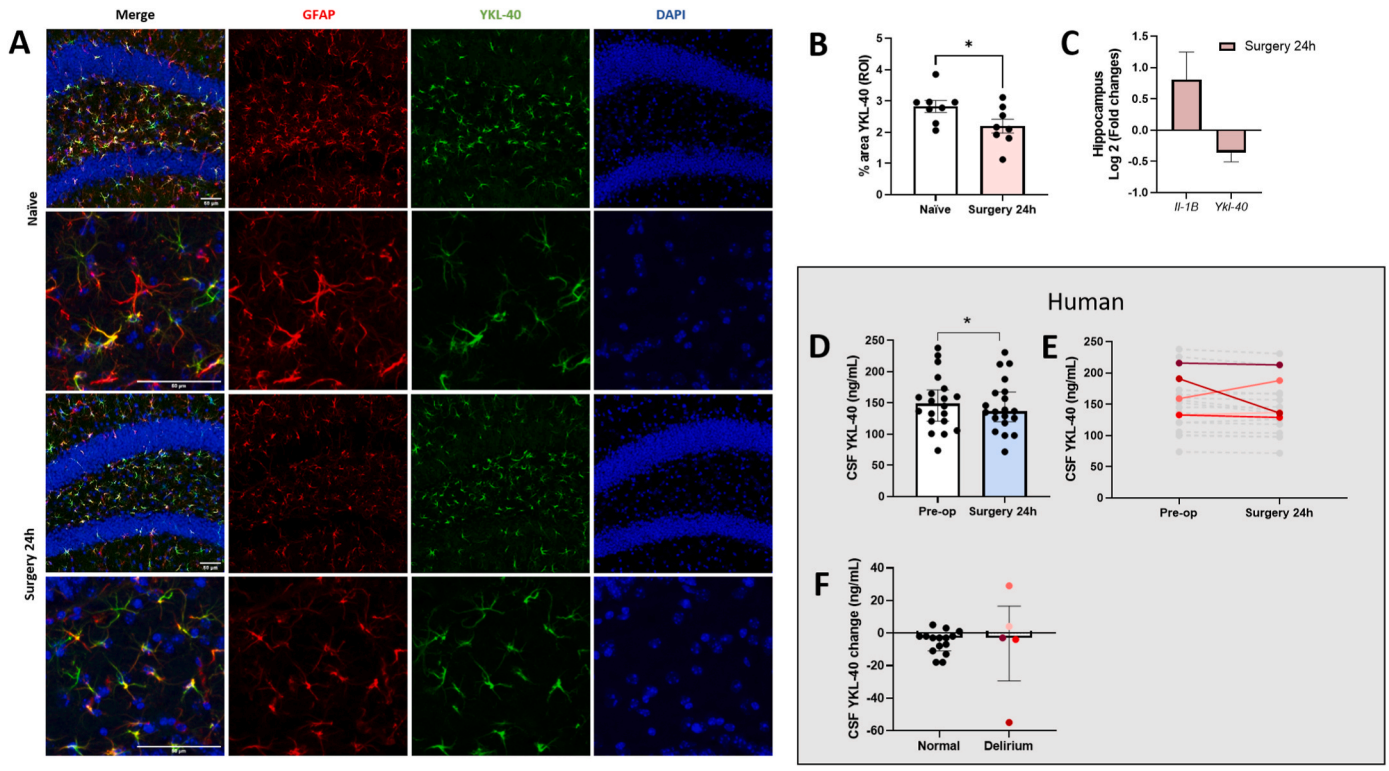

Fig. 2. CNS YKL-40 changes following surgery in mice and humans. Mouse brains were collected from aged mice 24 h following tibial fracture or from naïve unoperated control mice. A) Representative immunohistochemical images of YKL-40 protein expression in the dentate gyrus of the hippocampus. B) The percent area of YKL-40 immunostaining was lower in the tibial surgery mice vs naïve controls. C) RT-PCR of *Ykl*-40 mRNA expression expressed as log2 of fold changes in the hippocampus found that *Ykl-40* levels were reduced following tibial fracture. Interestingly, RT-PCR *Il1-B* log 2 of fold change in the hippocampus analysis showed increased *Il1-B* levels following tibial fracture. D) YKL-40 levels in CSF samples from human surgery patients examined before and 24 h after surgery revealed a significant decrease in YKL-40 in the CSF following surgery. E) Individual patient's preoperative and postoperative levels are represented in grey (normal) or colored (patients with delirium). F) Patients were divided into 2 groups: normal and patients with delirium. CSF YKL-40 change levels (24 h vs preoperative) between normal and patients with delirium. Mouse data are expressed as mean ± SEM, and human data as mean ± SD except for CSF YKL-40 data, which are expressed as Median ± (interquartile range). Analyses were performed as follows: Unpaired Student's *t*-test, Wilcoxon Rank Sum Test when appropriate, *p < 0.05. Representative scale for A) is 50 μm. Note: Individual dot colors represent the same patient with delirium across panels E and F. . (For interpretation of the references to color in this figure legend, the reader is referred to the Web version of this article.)

(Fig. 3D). Together with YKL-40, we also observed elevated plasma IL-6: Naïve mean: 8.828 pg/mL (SEM: 4.358), Surgery mean: 55.10 pg/mL (SEM: 4.879); Student's *t*-test; ($p < 0.0001$; MD = 46.28, 95% CI [32.02, 60.53]) (Fig. 3E), which is consistent with prior work using this mouse model and a study on human plasma from patients with delirium (Hu et al., 2018) (Hirsch et al., 2016).

3.6. Changes in NfL and BBB opening after surgery in mice

Using the same murine plasma samples, we performed SIMOA analyses of NfL. Given the peak of inattention and established neuroinflammation on postoperative day 1, we evaluated NfL at this time. Plasma levels of NfL were significantly increased 24 h after tibial fracture: Naïve mean: 153.3 pg/mL (SEM: 15.94), Surgery mean: 755.1 pg/mL (SEM: 57.36); Student's *t*-test; ($p < 0.0001$; MD = 601.8, 95% CI [472, 731.5]) (Fig. 4A). Although we did not investigate the origin of NfL in the current study, we observed that the BBB was significantly impaired in the aged mice after surgery, suggesting a possible way for brain-derived NfL to enter the bloodstream. In fact, loss of key mRNA tight-junction markers was evident as early as 9 h after surgery, and was still impaired 24 h post tibial fracture surgery (*occludin*, *Cd31*, *Zo1*, *claudin 5* and *Aq-4*) by RT-PCR (Fig. 4B).

In addition, we used immunohistochemistry to evaluate expression of the astrocytic end-foot and BBB integrity marker AQ-4 and the endothelial cell marker CD31. AQ-4 protein immuno-reactivity expression in the dentate gyrus ROI was decreased 24 h after surgery: Naïve mean: 6.473 (SEM: 0.197), Surgery mean: 5.587 (SEM: 0.2955); Student's *t*-test; ($p = 0.0258$; MD = −0.8854, 95% CI [−1.647, −0.1237]) (Fig. 4D). Similarly, CD31 protein immuno-reactivity expression was reduced at the 24-h timepoint: Naïve mean: 6.958 (SEM: 0.3183), Surgery mean: 6.05 (SEM: 0.2283); Student's *t*-test; ($p = 0.0346$; MD = −0.9074, 95% CI [−1.738, −0.07679]) (Fig. 4F).

4. Discussion

This project aimed to compare neuroimmune endpoints relevant to delirium pathophysiology in mice *vs* humans after surgery. We described a conserved YKL-40 response to anesthesia and surgery, with an increase in plasma levels but a decrease in CNS levels in both mice and humans. Notably, evaluation of YKL-40 expression in the mouse brain revealed a significant decrease in YKL-40 in hippocampal astrocytes after surgery. This raises the possibility that a similar decrease in CNS YKL-40 expression occurs following surgery in humans, which would fit with the decrease in YKL-40 levels in human CSF that we observed following surgery. In mice, we also found a significant increase in plasma NfL after surgery, which was associated with BBB breakdown. These findings advance our understanding of the dysfunctional cellular and molecular processes that may contribute to postoperative delirium pathogenesis in the aging brain.

This study leveraged complementary multi-species assays to clarify neuroimmune mechanisms in postoperative delirium. In fact, by using a subset of the well-phenotyped INTUIT cohort with parallel plasma and

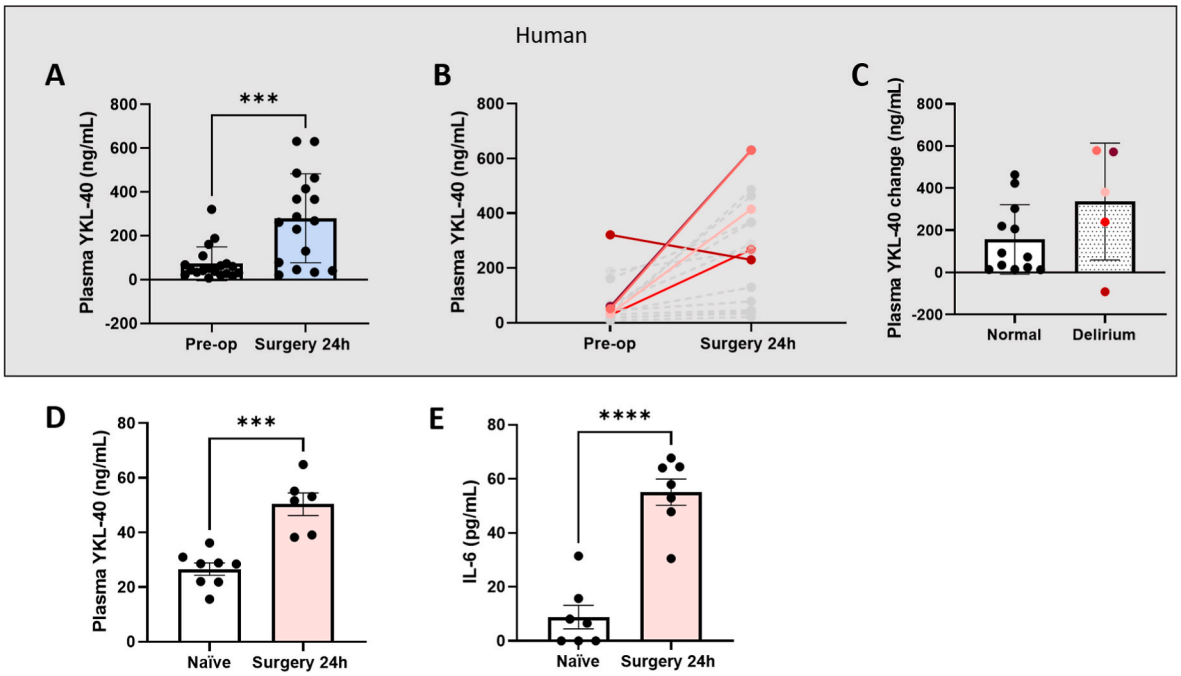

Fig. 3. Plasma YKL-40 changes following surgery in humans and mice. A) Human plasma concentrations of YKL-40 revealed increased levels following surgery when compared to preoperative levels within the same patients. B) Individual patient preoperative and postoperative levels are represented in grey (normal) or colored (patients with delirium). C) A trend toward increase was observed in plasma YKL-40 change levels (24 h vs preoperative) between normal and patients with delirium. D) Mouse plasma samples were collected from aged mice 24 h following tibial fracture or from naïve control mice. A similar increase in mouse plasma YKL-40 was observed 24 h following surgery. E) Plasma IL-6, a marker of inflammation, revealed that aged mice had increased inflammation 24 h after surgery. Human data are expressed as mean ± SD, and mouse data as mean ± SEM. Analyses were performed as follows: Paired and Unpaired Student's t-test when appropriate, ***$p < 0.001$. Note: Individual dot colors represent the same patient with delirium across panels B and C. . (For interpretation of the references to color in this figure legend, the reader is referred to the Web version of this article.)

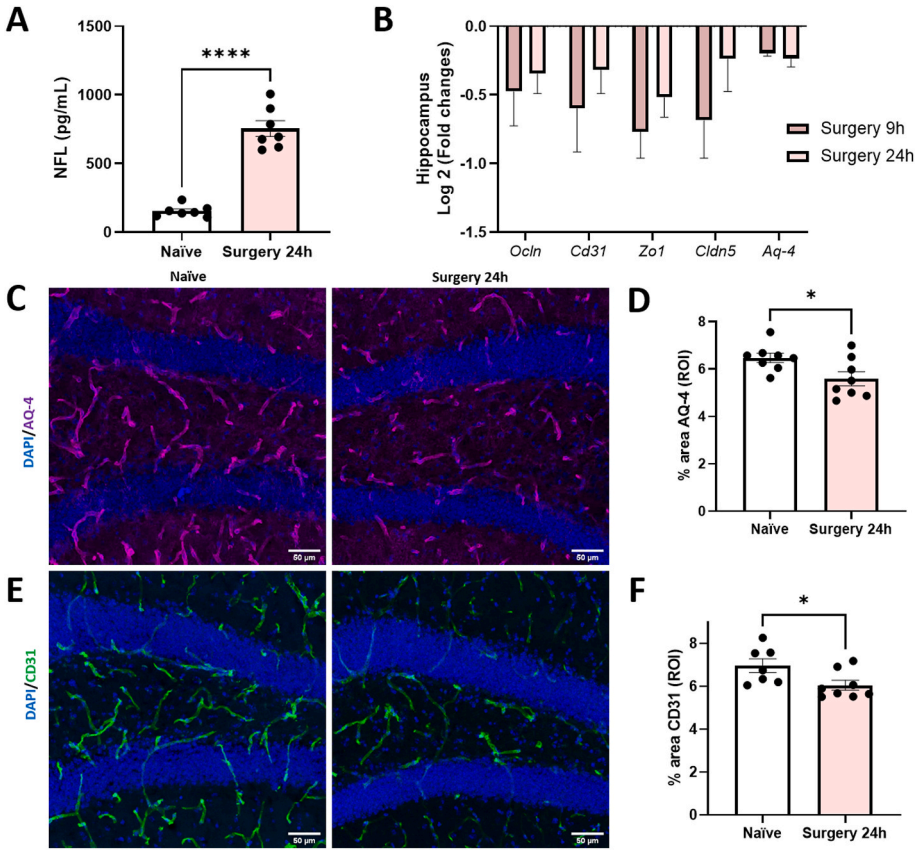

Fig. 4. BBB impairments following surgery. Brains were collected from aged mice 24 h following tibial fracture or from naïve control mice. A) Using Quanterix Simoa, plasma NfL, a marker of neuronal damage, revealed that aged mice had increased levels 24 h after surgery. B) RT-PCR log 2 of fold changes of Occludin, Cd31, Zo1, Claudin5, and Aq-4 revealed BBB impairment at 9 and 24 h following tibial fracture. C) Representative images of the astrocytic endfeet AQ-4 and E) the endothelial cell marker CD31 revealed decreased percentage area covered by D) AQ-4 and F) CD31 staining in the dentate gyrus following orthopedic surgery. Data expressed as mean ± SEM, *$p < 0.05$. Analyses were performed as follows: Unpaired Student's t-test. Representative scale for C, E) is 50 μm.

CSF analyses, together with a mouse model of orthopedic surgery, we have described remarkable similarities in the neuroimmune response to anesthesia and surgery. We have particularly focused on YKL-40 due to the growing evidence for its role in AD neurodegeneration as well as postoperative delirium. Recently, Vasunilashorn et al. (2022) described plasma YKL-40 as a key delirium-associated protein both as a risk marker for delirium (ie, preoperative elevation) and as a disease marker that is increased more in delirious patients on postoperative day 2 than in non-delirious patients. In their proteome-wide analysis of plasma from 18 older orthopedic surgery patients with postoperative delirium and 18 matched controls, Vasunilashorn et al. identified YKL-40 as the only protein among >1300 evaluated with preoperative elevation that predicted delirium and a postoperative elevation trend that followed delirium onset and possibly, resolution (Vasunilashorn et al., 2022). These findings, suggesting that YKL-40 may be a useful plasma biomarker for delirium, are not surprising as YKL-40 has been associated with ICU mortality in sepsis (Kornblit et al., 2013), prion disease (Llorens et al., 2017; Villar-Piqué et al., 2019), AD, and other dementias (vascular, Lewy body, fronto-temporal) (Llorens et al., 2017; Kornblit et al., 2013); however, plasma YKL-40 levels cannot definitively link central YKL-40 to delirium. We found that plasma YKL-40 changes are consistent with prior reports in our clinical cohort, although we were underpowered to detect changes in delirious subjects. Based on the level of variability in the 24-h change in plasma YKL-40 observed in the human samples (212 ng/mL), a future human study with a 12% delirium incidence would require 297 subjects (36 with and 261 without delirium) to detect a Cohen's effect size of 0.50. Based on the 24-h plasma YKL-40 increase of 156.7 ng/mL in our human subjects without delirium, such a study would be able to detect a 1.68 times higher YKL-40 increase (263 ng/mL) among those who develop delirium.

Interestingly, we found a similar response in aged mice after surgery, suggesting that a YKL-40 increase in the periphery is likely a conserved response to tissue injury, possibly mediated by peripheral immunocytes (Schultz and Johansen, 2010). However, for both mice and humans, the YKL-40 response in the CNS was surprising, and opposite from what we found in plasma. In fact, CSF YKL-40 levels were lower 24 h after surgery, with no detectable difference between subjects that had delirium. In (Vasunilashorn et al., 2021), no changes were observed in CSF YKL-40 postoperatively, possibly explaining a different etiology compared to other neurodegenerative conditions with robustly elevated YKL-40 in the CSF (Llorens et al., 2017; Craig-Schapiro et al., 2010; Kornblit et al., 2013; Villar-Piqué et al., 2019; Alcolea et al., 2017; Bonneh-Barkay et al., 2010; Emre et al., 2020; Falcon et al., 2019; Lananna et al., 2020; Woollacott et al., 2020). In the CNS, astrocytes are the primary source of YKL-40, which provides an attractive target for treating AD (Zhang et al., 2016).

Here, we evaluated astrocyte pathology in the mouse hippocampus, and confirmed reduced YKL-40 expression both at mRNA and protein levels 24 h after orthopedic surgery. At this timepoint, GFAP + astrocytes were visibly dystrophic, and YKL-40 expression was mostly confined within these cells. It is possible that YKL-40 requires more time to become upregulated in the CNS, given that delirium is characterized by a rapid and acute onset. Astrocyte dysfunction in this model was previously described (Femenía et al., 2017), suggesting a role not only for neuroinflammation but also for neurometabolic dysfunction in delirium. In fact, levels of *Il-1β* mRNA expression were increased even though *Ykl*-40 mRNA expression was reduced at 24 h, possibly contributing to prolonged astrocyte pathology in the vulnerable brain (Lopez-Rodriguez et al., 2021; Hennessy et al., 2015). Overall, the murine evidence suggests that the postoperative human decrease in CSF YKL-40 levels truly reflects central processes.

Astrocytes are also important regulators of the BBB (Kadry et al., 2020). In this study, we confirmed the loss of astrocytic end-feet processes and endothelial markers at 24 h after surgery in mice, suggesting that BBB opening is a major culprit for ensuing delirium-like behavior (Yang, 2022). Here, we confirmed the validity of another plasma biomarker that is upregulated in delirious subjects: NfL (Casey et al., 2019; Fong et al., 2020). The abundance of NfL in plasma together with early signs of BBB opening may indicate a central source for this neuronal injury marker. The ability to interrogate CNS damage via systemic biofluids is highly tractable in the clinic; however, peripheral nerve damage itself could contribute to the cellular source of NfL in plasma. Further characterization of this cellular response is needed not only in delirium but also in AD and other AD-related dementias.

Importantly, these data support the notion that delirium biomarkers are dynamic. These dynamic biomarkers may not represent the global cognitive changes that manifest in this syndrome. For example, BBB changes are limited to select areas of vulnerability, suggesting that only particular regions of interests are susceptible to anesthesia and surgery. This explains why molecules, including peripheral YKL-40, do not passively diffuse across a permeable BBB. While plasma biomarkers are undoubtedly more accessible and feasible in human clinical medicine than CSF biomarkers, they must be interpreted cautiously. This need for caution is apparent in our findings that plasma YKL-40 increases, while CSF and murine data suggest a central YKL-40 decrease. One means to guide and enrich plasma biomarker interpretation is to evaluate these markers in alternative models, such as with parallel human CSF analysis and/or the trans-species model with murine histology and RT-PCR analysis presented here. Overall, the differential change observed in plasma and CSF YKL-40 suggests cautious use of plasma biomarkers that may not specifically reflect brain changes. More broadly, this study encourages evaluation of possible alternative sources of plasma biomarkers, and provides a rationale for the importance of evaluating BBB integrity.

Further, we demonstrated ways to study delirium mechanisms using parallel human and rodent models. For example, the attention deficit characterized in the 5-CSRTT in mice is homologous to the inattention delirium sub-feature observed in human patients, and our results facilitates translational studies between mice and humans (Velagapudi et al., 2019). Animals subjected to tibial fracture have decreased performance on the 5-CSRTT within 24 h after surgery compared to sham controls. Moreover, even though the mice that underwent surgery exhibited some recovery exemplified by increased success rates over subsequent test days, these animals still remained below the performance levels of the sham controls at various time-points after surgery. Besides being deficient on recovery of attention performance, postoperative mice also required more time to respond to the 1.5 s visual stimulus than the sham controls. This prolonged latency to respond suggests that information processing for attention or other processes may be impaired in the surgical mice.

Notably, we also report increased plasma NfL levels post tibial fracture surgery in mice, which parallels similar reports in delirious older patients after surgery (Casey et al., 2019; Fong et al., 2020). In humans, there are also limitations to studying neuronal activation at a cellular level; however, in this study using FosTRAP mice, we showed PLC neuronal activation post tibial fracture in mice. This result links the behavior observed in the human delirium phenotype (decreased attention) with a potential neuronal mechanism (PLC neuronal activation) in mice that can only practically and ethically be examined in animal models. Collectively, this cross-species evaluation allowed us to use histology to fill in the gaps necessitated by human biomarker studies while grounding our pre-clinical models with parallel data samples from human patients.

4.1. Limitations

There are a few limitations to this study. The breeding time required for FosTRAP mice and the complexity of tamoxifen-induced recombination (e.g., successive daily injections required in older mice) made the use of older mice for the FosTRAP experiments impossible for this specific study. Attentional and delirium evaluations in both mice and

humans focused on the 24-h post-surgery time-point when inattention peaked in the 5-CSRTT and while all human subjects were still hospitalized and thus, available for 3D-CAM assessment. Future studies should characterize the long-term cognitive sequelae of surgery and/or delirium. We used a limited number of human patients with and without delirium to confirm our findings in mice. In addition, human patients were not randomly chosen as they were selected for *APOE4*-carrier status in conjunction with a separate project. Therefore, there is an overrepresentation of *APOE4* carriers in this cohort. Finally, the available human samples in this study came from patients who underwent various types of non-cardiac non-neurologic surgery, while the rodent model only replicated orthopedic injury/surgery. Despite the breath of procedures, these data imply that sufficient homology is present between species following different surgical manipulations. Thus, cross-species postoperative delirium models likely do not require identical rodent and human surgeries, just as clinical delirium research often includes patients undergoing many different surgery types.

5. Conclusion

In this study, we confirmed that plasma biomarkers associated with human delirium are also elevated in mice postoperatively. We built on those human findings with a more in-depth histologic analysis of transgenic FosTRAP mice and with mRNA expression assessments. Human retrospective studies have shown that patients who develop postoperative delirium or sustain other neurologic injuries (eg, traumatic brain injury) tend to have higher levels of plasma biomarkers associated with astrocyte function, general inflammation, and neuronal injury. In this study, we showed that levels of the plasma inflammatory marker IL-6 increased at 24 h post tibial fracture surgery in mice. Although we did not measure IL-6 in humans here, given that inflammation occurs after any trauma including surgery, and that massive systemic inflammation in sepsis often occurs with delirium, previous studies revealed that the inflammatory marker IL-6 is significantly higher in the plasma of postoperative patients who develop delirium compared with those who do not develop delirium (Chen et al., 2019; Lv et al., 2021). Overall, this cross-species study using complementary mouse and human preparations yielded novel insights that neither a rodent nor human study could produce independently. We demonstrated a conserved YKL-40 response (increases peripherally and decreases centrally) among aged mice following orthopedic surgery and older human surgery patients. These findings urge cautious interpretation of plasma delirium biomarkers considering evidence for BBB compromise and unanticipated peripheral biomarker sources.

Author contributions

JD, LA, AC, YW, and SG performed experiments and analyzed data; NF, RMR, and WW conducted and analyzed the behavioral study; MCW overviewed the statistical analyses; MD, HZ, and TY contributed key reagents; MB supervised the human study; and NT, JD, and LA conceived the idea. JD, LA, MB, and NT wrote the manuscript with input from all authors. All authors read and approved the manuscript.

Declaration of competing interest

HZ has served on scientific advisory boards and/or as a consultant for Abbvie, Acumen, Alector, ALZPath, Annexon, Apellis, Artery Therapeutics, AZTherapies, CogRx, Denali, Eisai, Nervgen, Novo Nordisk, Passage Bio, Pinteon Therapeutics, Red Abbey Labs, reMYND, Roche, Samumed, Siemens Healthineers, Triplet Therapeutics, and Wave, has given lectures in symposia sponsored by Cellectricon, Fujirebio, Alzecure, Biogen, and Roche, and is a co-founder of Brain Biomarker Solutions in Gothenburg AB (BBS), which is a part of the GU Ventures Incubator Program (outside submitted work).

Data availability

Data will be made available on request.

Acknowledgements

We would like to acknowledge the Duke Molecular Physiology Institute Molecular Genomics Core for generating the NfL data (RRID: SCR_017860), the Duke Behavioral Core (Christopher Means), the Duke Microscopy Core (Lisa Cameron and Benjamin Carlson), Fan Wang (MIT) for her gift of the Fos-TRAP mice and Kathy Gage for editorial assistance.

LA acknowledges support from NIH T32GM008600. NT acknowledges support from National Institutes of Health grants R01-AG057525 and P01-AT009968-A1, Alzheimer's Association (2019-AARG-643070), and the Duke Department of Anesthesiology. HZ is a Wallenberg Scholar supported by grants from the Swedish Research Council (#2018–02532), the European Union's Horizon Europe research and innovation programme under grant agreement No 101053962, Swedish State Support for Clinical Research (#ALFGBG-71320), the Alzheimer Drug Discovery Foundation (ADDF), USA (#201809–2016862), the AD Strategic Fund and the Alzheimer's Association (#ADSF-21-831376-C, #ADSF-21-831381-C, and #ADSF-21-831377-C), the Bluefield Project, the Olav Thon Foundation, the Erling-Persson Family Foundation, Stiftelsen för Gamla Tjänarinnor, Hjärnfonden, Sweden (#FO 2022-0270), the European Union's Horizon 2020 research and innovation programme under the Marie Skłodowska-Curie grant agreement No 860197 (MIRIADE), the European Union Joint Programme – Neurodegenerative Disease Research (JPND 2021-00694), and the UK Dementia Research Institute at UCL (UKDRI-1003).

Appendix A. Supplementary data

Supplementary data to this article can be found online at https://doi.org/10.1016/j.bbih.2022.100555.

References

Alcolea, D., et al., 2017. CSF sAPPβ, YKL-40, and neurofilament light in frontotemporal lobar degeneration. Neurology 89 (2), 178–188.
Berger, M., et al., 2019. The INTUIT study: investigating neuroinflammation underlying postoperative cognitive dysfunction. J. Am. Geriatr. Soc. 67 (4), 794–798.
Bichot, N.P., et al., 2015. A source for feature-based attention in the prefrontal cortex. Neuron 88 (4), 832–844.
Bonneh-Barkay, D., et al., 2010. In vivo CHI3L1 (YKL-40) expression in astrocytes in acute and chronic neurological diseases. J. Neuroinflammation 7 (1), 34.
Breyne, K., et al., 2018. Immunomodulation of host chitinase 3-like 1 during a mammary pathogenic Escherichia coli infection. Front. Immunol. 9.
Casey, C.P., et al., 2019. Postoperative delirium is associated with increased plasma neurofilament light. Brain 143 (1), 47–54.
Chen, Y., et al., 2019. Change in serum level of interleukin 6 and delirium after coronary Artery bypass graft. Am. J. Crit. Care 28 (6), 462–470.
Craig-Schapiro, R., et al., 2010. YKL-40: a novel prognostic fluid biomarker for preclinical Alzheimer's disease. Biol. Psychiatr. 68 (10), 903–912.
David, J., et al., 2019. L-alpha-amino adipic acid provokes depression-like behaviour and a stress related increase in dendritic spine density in the pre-limbic cortex and hippocampus in rodents. Behav. Brain Res. 362, 90–102.
De, J., Wand, A.P., 2015. Delirium screening: a systematic review of delirium screening tools in hospitalized patients. Gerontol. 55 (6), 1079–1099.
DeNardo, L.A., et al., 2019. Temporal evolution of cortical ensembles promoting remote memory retrieval. Nat. Neurosci. 22 (3), 460–469.
Emre, C., et al., 2020. Receptors for pro-resolving mediators are increased in Alzheimer's disease brain. Brain Pathol. 30 (3), 614–640.
Evered, L., et al., 2022. Acute peri-operative neurocognitive disorders: a narrative review. Anaesthesia 77 (S1), 34–42.
Falcon, C., et al., 2019. CSF glial biomarkers YKL40 and sTREM 2 are associated with longitudinal volume and diffusivity changes in cognitively unimpaired individuals. Neuroimage Clin 23, 101801.
Femenía, T., et al., 2017. Disrupted neuro-glial metabolic coupling after peripheral surgery. J. Neurosci. 38 (2), 452–464.
Fingar, K., Stocks, C., Weiss, A., Steiner, C., 2014. Most Frequent Operating Room Procedures Performed in U.S. Hospitals, 2003-2012. U.D.o.H.a.H.S. Agency for Healthcare Research and Quality.

Fong, T.G., et al., 2020. Association of plasma neurofilament light with postoperative delirium. Ann. Neurol. 88 (5), 984–994.
Gou, R.Y., et al., 2021. One-Year Medicare Costs Associated with Delirium in Older Patients Undergoing Major Elective Surgery. JAMA Surg.
Guenthner, C.J., et al., 2013. Permanent genetic access to transiently active neurons via TRAP: targeted recombination in active populations. Neuron 78 (5), 773–784.
Healy, S., et al., 2018. Threshold-based segmentation of fluorescent and chromogenic images of microglia, astrocytes and oligodendrocytes in Fiji. J. Neurosci. Methods 295, 87–103.
Hennessy, E., Griffin, É.W., Cunningham, C., 2015. Astrocytes are primed by chronic neurodegeneration to produce exaggerated chemokine and cell infiltration responses to acute stimulation with the cytokines IL-1β and TNF-α. J. Neurosci. 35 (22), 8411–8422.
Hirsch, J., et al., 2016. Perioperative cerebrospinal fluid and plasma inflammatory markers after orthopedic surgery. J. Neuroinflammation 13 (1), 211.
Hu, J., et al., 2018. Interleukin-6 is both necessary and sufficient to produce perioperative neurocognitive disorder in mice. Br. J. Anaesth. 120 (3), 537–545.
Inouye, S.K., Westendorp, R.G.J., Saczynski, J.S., 2014. Delirium in elderly people. Lancet 383 (9920), 911–922.
Kadry, H., Noorani, B., Cucullo, L., 2020. A blood-brain barrier overview on structure, function, impairment, and biomarkers of integrity. Fluids Barriers CNS 17 (1), 69.
Kornblit, B., et al., 2013. Plasma YKL-40 and CHI3L1 in systemic inflammation and sepsis-experience from two prospective cohorts. Immunobiology 218 (10), 1227–1234.
Lananna, B.V., et al., 2020. Chi3l1/YKL-40 is controlled by the astrocyte circadian clock and regulates neuroinflammation and Alzheimer's disease pathogenesis. Sci. Transl. Med. 12 (574), eaax3519.
Livak, K.J., Schmittgen, T.D., 2001. Analysis of relative gene expression data using real-time quantitative PCR and the 2(-Delta Delta C(T)) Method. Methods 25 (4), 402–408.
Llorens, F., et al., 2017. YKL-40 in the brain and cerebrospinal fluid of neurodegenerative dementias. Mol. Neurodegener. 12 (1), 83.
Lopez-Rodriguez, A.B., et al., 2021. Acute systemic inflammation exacerbates neuroinflammation in Alzheimer's disease: IL-1β drives amplified responses in primed astrocytes and neuronal network dysfunction. Alzheimers Dement 17 (10), 1735–1755.
Lv, X.C., et al., 2021. Plasma interleukin-6 is a potential predictive biomarker for postoperative delirium among acute type a aortic dissection patients treated with open surgical repair. J. Cardiothorac. Surg. 16 (1), 146.
Marcantonio, E., et al., 2014. 3D-CAM: derivation and validation of a 3-minute diagnostic interview for CAM-defined delirium. Ann. Intern. Med. 161, 554–561.
Masutani, R., et al., 2020. Outcomes of common major surgical procedures in older adults with and without dementia. JAMA Netw. Open 3 (7), e2010395-e2010395.
Nobuhara, C.K., et al., 2020. A protocol to reduce self-reported pain scores and adverse events following lumbar punctures in older adults. J. Neurol. 267 (7), 2002–2006.
Schultz, N.A., Johansen, J.S., 2010. YKL-40-a protein in the field of translational medicine: a role as a biomarker in cancer patients? Cancers 2 (3), 1453–1491.
Squire, R.F., et al., 2013. Prefrontal contributions to visual selective attention. Annu. Rev. Neurosci. 36 (1), 451–466.
Taylor, J., et al., 2022. Postoperative delirium and changes in the blood-brain barrier, neuroinflammation, and cerebrospinal fluid lactate: a prospective cohort study. Br. J. Anaesth. 129 (2), 219–230.
Vasunilashorn, S.M., et al., 2020. A new severity scoring scale for the 3-minute confusion assessment method (3D-CAM). J. Am. Geriatr. Soc. 68 (8), 1874–1876.
Vasunilashorn, S.M., et al., 2021. Plasma and cerebrospinal fluid inflammation and the blood-brain barrier in older surgical patients: the Role of Inflammation after Surgery for Elders (RISE) study. J. Neuroinflammation 18 (1), 103.
Vasunilashorn, S.M., et al., 2022. Proteome-wide analysis using SOMAscan identifies and validates chitinase-3-like protein 1 as a risk and disease marker of delirium among older adults undergoing major elective surgery. J Gerontol A Biol Sci Med Sci 77 (3), 484–493.
Velagapudi, R., et al., 2019. Orthopedic surgery triggers attention deficits in a delirium-like mouse model. Front. Immunol. 10, 2675.
Villar-Piqué, A., et al., 2019. Plasma YKL-40 in the spectrum of neurodegenerative dementia. J. Neuroinflammation 16 (1), 145.
Wang, P., et al., 2020. Neurovascular and immune mechanisms that regulate postoperative delirium superimposed on dementia. Alzheimers Dement 16 (5), 734–749.
Wilson, J.E., et al., 2020. *Delirium.* Nature Reviews Disease Primers 6 (1), 90.
Woollacott, I.O., et al., 2020. Cerebrospinal fluid YKL-40 and chitotriosidase levels in frontotemporal dementia vary by clinical, genetic and pathological subtype. Dement. Geriatr. Cognit. Disord. 49 (1), 56–76.
Yang, T., et al., 2022. Protective effects of omega-3 fatty acids in a blood–brain barrier-on-chip model and on postoperative delirium-like behaviour in mice. Br. J. Anaesth. https://doi.org/10.1016/j.bja.2022.05.025. In press.
Zhang, Y., et al., 2016. Purification and characterization of progenitor and mature human astrocytes reveals transcriptional and functional differences with mouse. Neuron 89 (1), 37–53.